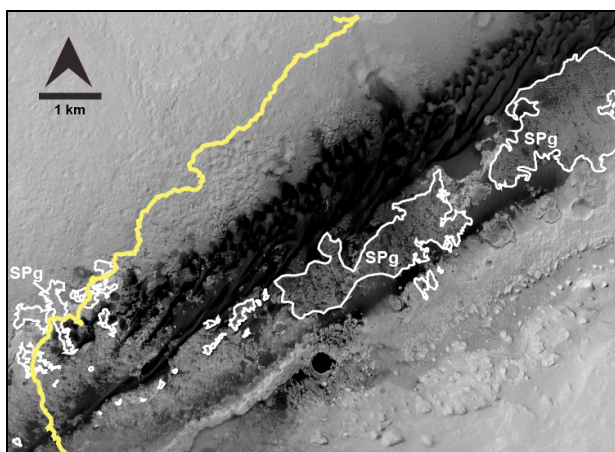


**FORMATION OF FRACTURE NETWORKS IN THE SICCAR POINT GROUP: IMPLICATIONS FOR TIMING OF POST-DEPOSITIONAL FLUID FLOW IN GALE CRATER, MARS.** R.E. Kronyak<sup>1\*</sup>, L.C. Kah<sup>1</sup>, N.B. Miklusicak<sup>1</sup>, K.S. Edgett<sup>2</sup>, M. Nachon<sup>3</sup>, C.M. Fedo<sup>1</sup>, <sup>1</sup>Department of Earth and Planetary Sciences, University of Tennessee, Knoxville, TN, [\\*rkronyak@vols.utk.edu](mailto:rkronyak@vols.utk.edu), <sup>2</sup>Malin Space Sciences Systems, San Diego, CA, <sup>3</sup>University of California, Davis, CA.

**Introduction:** Mineralized fractures are common features in the strata that comprise Aeolis Mons (Mount Sharp), Gale crater. Such mineralization is expressed across multiple scales. Sub-millimeter to centimeter-thick veins have been observed along Curiosity's ~18 km traverse from Yellowknife Bay to the rover's current position atop the Vera Rubin Ridge [1]. In addition, decameter-scale resistant networks of cemented fractures have been observed in images acquired from orbit on the slopes of Mount Sharp [2].

The widespread nature of these fracture networks suggests potential for substantial post-depositional fluid flow. However, the timing and number of fluid events remain uncertain. Here we explore the distribution of mineralized fractures in strata exposed on the lower slopes of Mount Sharp, observable in MRO HiRISE images, to better understand the nature and extent of post-depositional fluid flow (Fig. 1).



**Figure 1.** Mosaic of HiRISE images showing the northern slope of Lower Mount Sharp. Curiosity's traverse is outlined in yellow and areas of exposed SPg in white.

#### Fracture observations:

**Curiosity veins and fractures:** From the ground, data from Curiosity have provided evidence for subsurface fluid flow by the presence of mineral veins and alteration halos. The veins observed thus far are primarily composed of Ca-sulfate and are most abundant in the Murray formation. These veins are hypothesized to have formed by hydrofracturing processes. Evidence for hydrofracturing includes changes in vein aperture, particularly near a capping lithology, suggesting locally elevated fluid pressures; and penetration of veins

into, but not completely through, highly cemented capping units, indicating fluid pressures sufficient to allow propagation across a stress barrier, followed by arrest as fracture energy dissipates [3]. Observations of multigenerational, crack-seal vein fills provide additional evidence for multiple pulses of elevated fluid pressures and reopening of pre-existing fractures.

In the Stimson formation, Ca-sulfate veins are present but minor, and additional evidence for migration of subsurface fluid exists in the presence of fracture-parallel alteration halos. The fractures do not preserve mineralized vein material and are potentially consistent with alteration by subsurface hydrothermal fluids that leached host rock around new and/or potentially pre-existing fractures [4].

**HiRISE: Siccar Point group:** Here we investigate a dense mineralized fracture network in the Siccar Point group (SPg). The SPg is a relatively high thermal inertia, erosional resistant unit that unconformably overlies strata of the Murray formation along the lowermost slopes of Mount Sharp [5, 6, 7]. The SPg is best exposed to the east of the Bagnold Dunes (Fig. 1), although intermittent exposures extend to the mesa-forming Murray Buttes that Curiosity traversed through on Sols ~1350-1450 (Fig. 1). Exposures of erosional resistant material investigated by Curiosity that are associated with the SPg have been informally designated as the Stimson formation. Elevation of the SPg and potentially associated lithologies ranges from approximately -4500 m to -4230 m, reflecting an unconformable depositional relationship atop eroded strata of Lower Mount Sharp.

East of the Bagnold Dunes, the SPg has an average thickness of ~3 meters [7] and is characterized by three stratigraphic horizons with distinct surface textures. The uppermost third of the SPg is strongly pitted by small craters; areas between craters are erosional smooth. The middle interval contains distinct parallel ridges that are oriented ENE, giving the SPg a characteristic "washboard" texture [6, 7]. Finally, the lowermost SPg is characterized by abundant positive relief, polygonal structures interpreted to represent mineralized fractures. These features are preserved within the basal SPg and do not extend into the middle or uppermost SPg intervals (Fig. 2).

The size of individual polygons varies but averages ~10 meters across. Intersection angles of polygons also

vary, but morphology remains relatively uniform throughout the exposed lower SPg. From satellite images, we are uncertain whether the positive relief results from mineral infill of fractures or preferential cementation of strata surrounding fractures.

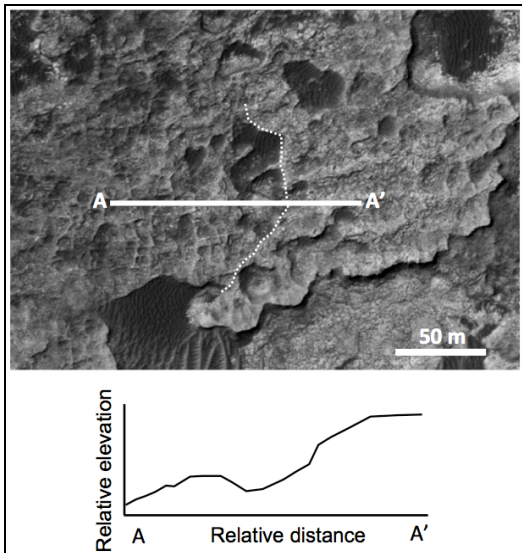


**Figure 2.** Portion of HiRISE image showing lower (A) and middle (A') horizons of the SPg. Polygonal fractures are restricted to the basal SPg.

Curiosity observed some of these features in the lower SPg in a long-range Mastcam mosaic pointed at a portion of the SPg from near Bradbury Landing (Sol 19; Fig. 3). This early view of the SPg shows white, erosional resistant linear features that appear to represent mineralized fractures. The nature of these features is not well constrained (e.g. Ca-sulfate veins vs. diagenetic halos). These features lack systematic orientations and show irregular intersections. Features are most apparent in the erosional resistant rocks of the lower SPg, although they extend in some places from the underlying Murray strata (Fig. 3).



**Figure 3.** Portion of Mastcam-right (M100) mosaic (mcam00054) taken on Sol 19 showing the SPg, where white lineations are observed to cross-cut dark gray caprock.

## Discussion

*Formation of fracture networks in the SPg:* Polygonal fractures have been previously reported in Gale

crater (boxwork structures of [2]). These features are interpreted to have formed from contractional stresses associated with desiccation and/or thermal processes [2]. In this case, tensional stresses result from repeated contraction and expansion of exposed lithified material within a relatively homogeneous applied stress field. Preferential cementation of host rock surrounding fractures is then inferred to result from migration of relatively shallow groundwater [2].

An alternative mechanism for the formation of polygonal fractures observed in the SPg is formation by overpressured subsurface fluids (i.e. hydrofracturing). Although typically a burial phenomenon, hydrofractures may form at any crustal depth, provided fluid pressures exceed rock strength. Fracturing here could reflect dissipation of energy associated with overpressured fluids within the underlying Murray formation. The absence of fracture propagation into overlying strata may then be attributed to dissipation of fluid pressures. In addition, applied stresses have a significant influence on the likelihood of fracture linkage. For example, under conditions of low differential stress (i.e. shallow burial), fractures have a stronger tendency to connect and intersect than in deeper regimes [8]. This, combined with homogeneity of the host rock material and/or isotropy of applied fluid pressure, might be sufficient to produce the observed polygonal fracture geometry in the SPg.

*Timing of fluid flow:* Although the formation mechanism of fracture networks in the SPg remains uncertain, the presence of features with erosive properties distinct from surrounding bedrock demands the presence of post-depositional fluid flow and secondary mineral precipitation (as vein fill or alteration within host rock). The presence of these mineral-associated fracture networks in the SPg requires regionally active fluid flow (surface or subsurface) following the deposition and lithification of the SPg, which occurs after both the deposition, lithification, and erosion of Mount Sharp.

## References:

- [1] Kronyak R. K., et al., (2017) *LPS XLVIII*, Abstract #1523. [2] Siebach K. L. and Grotzinger J. P. (2014) *JGR*, 119, 189-198. [3] Gudmundsson, A. (2011) University Press, Cambridge, 382-390. [4] Yen, A., et al. (2017) *EPSL* 471, 186-198. [5] Stack, K.M., et al., (2019) *LPS XLVIII*, Abstract #1889. [6] Anderson R. B. and Bell, J. F. III (2010) *Mars 5*, 76-128. [7] Kah L. C., et al. (2013) *LPS XLIV*, Abstract #1121. [8] Olson, J.E. and Pollard, D.D. (1991) *Journal of Structural Geology*, 13, 595-608.